

Article

Not peer-reviewed version

---

# Urban Land Use Characteristics and Heat Islands: A Spatial Analysis

---

[Asif Iqbal](#), [Md Mizanur Rahman](#)<sup>\*</sup>, [Chris Chow](#), [Peter Levett](#)

Posted Date: 21 August 2024

doi: 10.20944/preprints202408.1569.v1

Keywords: heat island; land use; spatial analysis; Landsat; Australia.; Normalised Difference Vegetation Index (NDVI)



Preprints.org is a free multidiscipline platform providing preprint service that is dedicated to making early versions of research outputs permanently available and citable. Preprints posted at Preprints.org appear in Web of Science, Crossref, Google Scholar, Scilit, Europe PMC.

Copyright: This is an open access article distributed under the Creative Commons Attribution License which permits unrestricted use, distribution, and reproduction in any medium, provided the original work is properly cited.

Article

# Urban Land Use Characteristics and Heat Islands: A Spatial Analysis

Asif Iqbal <sup>1</sup>, Md Mizanur Rahman <sup>1,\*</sup>, Chris Chow <sup>2</sup> and Peter Levett <sup>3</sup>

<sup>1</sup> UniSA STEM, University of South Australia, SA 5095, Australia

<sup>2</sup> SIRM, UniSA STEM, University of South Australia, SA 5095, Australia

<sup>3</sup> Infrastructure Delivery, the City of Salisbury, SA 5095, Australia

\* Correspondence: mizanur.rahman@unisa.edu.au

**Abstract:** The continuous expansion of urban areas has significantly increased the coverage of impervious paved surfaces, leading to heightened heat absorption and the formation of urban heat islands (UHIs). This research centres on environmental footprint accounting and management to address the escalating UHI risks in the City of Salisbury, Adelaide, South Australia. To comprehend the extent of land use change over time, the study employs the Normalised Difference Vegetation Index (NDVI) in conjunction with Landsat satellite maps. The satellite maps were also analysed for the historical land surface temperatures, exploring the correlation between land use change and land surface temperatures. This approach allows for exploring the correlation between land use transformations and UHI intensity. The re-search cross-referenced the satellite data with meteorological station records for verification, which led to identifying possible factors associated with the temperature change in the city. Furthermore, the research extends its scope by analysing aerial photography images of the city, enabling a comprehensive investigation of land cover contribution to UHI effects.

**Keywords:** heat island; land use; spatial analysis; landsat; Australia

## 1. Introduction

Urban areas have become increasingly important centres of economic, social, and cultural activity, attracting people from all walks of life. However, rapid urbanisation has also led to significant land use and cover changes, forming urban heat islands (UHIs). UHIs are characterised by higher temperatures in urban areas compared to their surrounding rural areas due to the absorption of solar radiation by urban surfaces such as buildings, pavements, and roads [1]. Urban heat islands (UHIs) are a significant phenomenon that has received increasing attention, especially as a footprint of land use change. As cities undergo rapid development and land use change, the impact on UHI intensity becomes a critical concern for sustainable urban planning, denoting the effect (footprint) of those developments/land uses. Several studies have shown that rapid urbanisation-led land use can significantly impact UHI intensity worldwide [2–4]. This research also intended to analyse land use changes over time, tracking the expansion of impervious surfaces to map the areas experiencing significant UHIs. However, this research focused more on the intensity of the effect and the analysis of other parameters that might affect the footprint.

UHI intensity is found higher in areas with a higher proportion of built-up land use than areas with more green space [5–10]. Thus, a city's land use change trajectories might also indicate the UHI trajectories [11–13]. However, the UHI effect might also vary seasonally for the same land use [14], signifying other factors that might influence the Land Surface Temperature (LST). The Normalised Difference Vegetation Index (NDVI) represents the extent of green space in land use, and numerous studies have investigated the relationship between NDVI and LST, two important indicators of UHI. Research has examined the relationship between NDVI and LST in the rapidly urbanising area of China and found that vegetation can mitigate the urban heat island effect [15–17] via

evapotranspiration. Lack of green spaces and choice of construction materials were found to impact LST in semi-arid regions significantly [18]. Urban vegetation also has a cooling effect on the built environment in subtropical desert cities, showing a strong inversely proportional relation between the oasis effect and NDVI [19]. Shades from buildings and big trees are found to have a cooling effect on paved surfaces, especially during summer, reducing the LST in those areas. However, trees were found to have a distinct effect when considered an option to mitigate urban heat [20]. The density of the vegetation is very important when considering reducing UHI effects through urban arboriculture. The research found that dense vegetation and large green spaces, having higher canopy areas, are more effective in reducing LST, than grasslands or scattered vegetation due to the effective reduction of temperature with evapotranspiration [21,22].

UHIs can cause a range of negative impacts, including increased energy consumption for cooling buildings, negative impacts on human health [23,24], and disruption of urban ecology [25]. For example, research has shown that UHIs can increase the frequency and severity of heat waves, leading to increased mortality rates among vulnerable populations such as the elderly and children [26–28]. UHIs can also disrupt urban ecosystems, with some plant and animal species being particularly sensitive to high temperatures [29,30]. In addition, UHIs contribute to climate change through increased energy consumption and greenhouse gas emissions [31–33]. Thus, UHIs are a significant issue for urban areas globally, with numerous negative impacts on human health, urban ecology, and the environment. Addressing UHIs requires various strategies that incorporate urban design, planning, and environmental management. Understanding the causes and impacts of UHIs is essential for developing effective policies and strategies that promote sustainable urban development and enhance the resilience of urban areas to climate change.

It is evident globally that vegetation land cover has a strong connection with the UHI, and, therefore, this research focused on a spatial analysis of the relationship between urban land use characteristics (in the form of NDVI) and UHIs for a developing city of South Australia (City of Salisbury). Such a case study area can more clearly portray the developments over the years. The research would be useful in identifying the extent of planning required (regarding vegetation) to mitigate urban heat from the Australian arid climate perspective. To aid the planning strategies, the research further aimed to examine the potential mitigating effects of green spaces and other urban design features on UHI intensity. Research has been conducted in Australia assessing the relations between historical land cover changes and surface temperatures [34–36]. However, research hasn't been conducted that can integrate the planning to combat the local scale climate. Thus, this research provides useful correlations, not only on the effect of land use change but also on the mitigation options and the consequences.

Remote sensing data and geographic information system (GIS) techniques were used to identify the spatial distribution of NDVI in the case study area and analyse its impact on the formation of UHIs. Landsat images have been increasingly used to study urban heat islands (UHIs) due to their ability to capture large-scale land use and land cover changes over time. Chen et al. investigated the spatiotemporal dynamics of UHIs over 17 years (2000-2017) using Landsat images in Wuhan, China [37]. Similarly, several research used Landsat images for analysing the relationships between the expansion of built-up areas and UHIs in Tehran (Iran), Hong Kong and Istanbul (Turkey) cities, justifying the wider acceptability of this approach, and was adopted in this research as well [38–41]. Further to the remote sensing analysis, meteorological data was analysed to understand better the relations, including the factors influencing the relations.

## **2. Materials and Methods**

### *2.1. Study Area*

Salisbury is a city located in the northern suburbs of Adelaide, South Australia (around 25 km north of Adelaide city). It covers an area of approximately 160 square kilometres and has a population of around 147,000 people [42].

The city of Salisbury is known for its cultural diversity and vibrant community. It is home to a wide range of amenities and attractions, including parks, shopping centres, restaurants, and

entertainment venues (Figure 1 for details). A significant portion of the City of Salisbury covers a conservation area, with more than 50 wetlands, open space and recreation facilities.

Over the years, Salisbury has also become home to several schools and educational institutions, including the University of South Australia's Mawson Lakes Campus and a campus of TAFE SA. The well-connected transport network to Adelaide via public transport, including bus and train services, has made the city a popular destination for living.

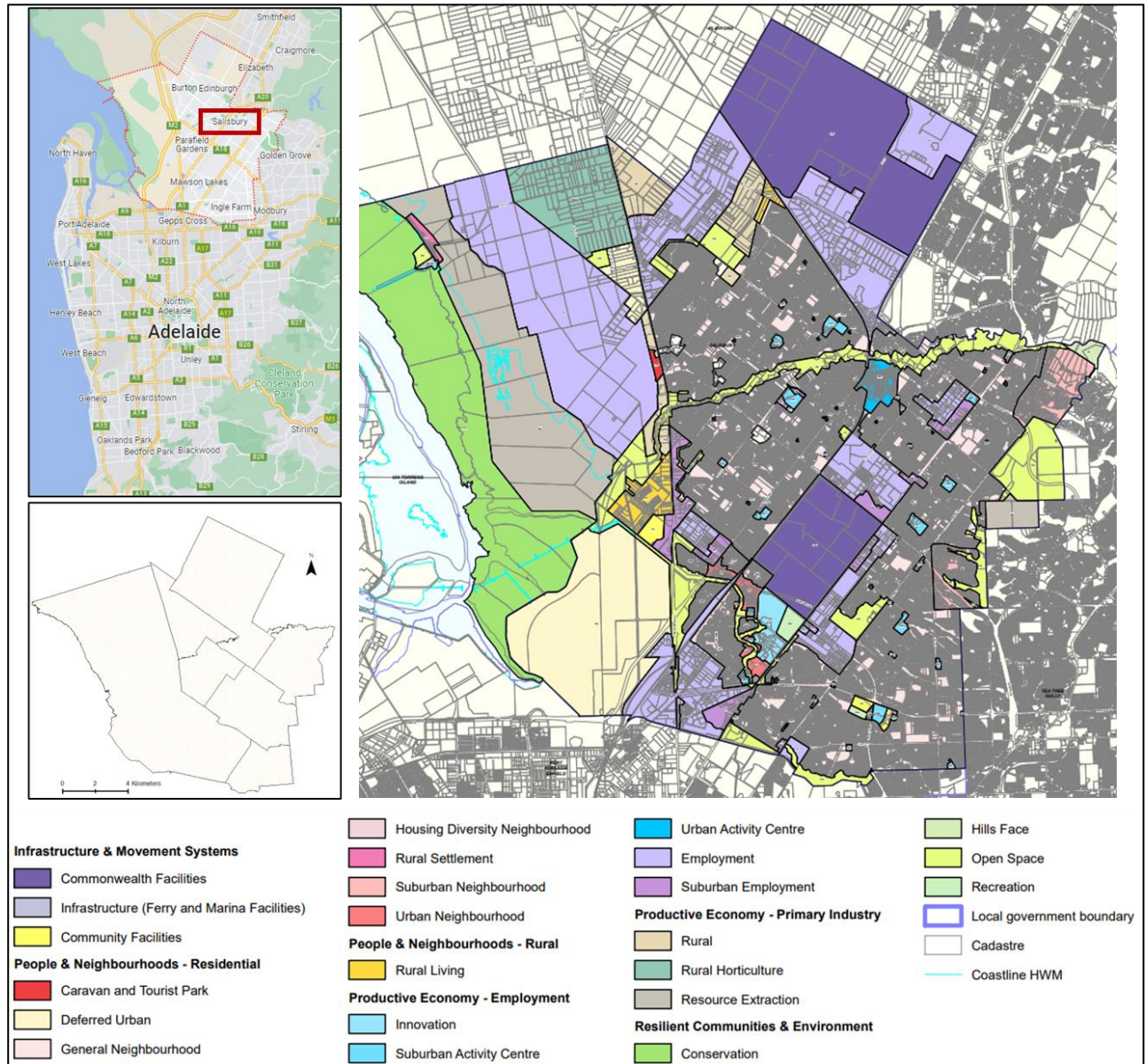


**Figure 1.** City of Salisbury maps located in the Greater Adelaide area of South Australia, indicating the city boundary and different land uses. Maps adapted from google maps [43], and PlanSA [44].

## 2.2. Data Collection

To investigate urban heat islands effects, three way analysis was conducted by analysing the land use and land cover changes through satellite maps, assessing the significance of meteorological conditions, and investigating the magnitude of land cover effects through aerial photographs.

### a. Satellite maps

Landsat satellite images were collected for 23 years (1997 – 2020) for land use and LST analysis. Because of the high-altitude acquisition of the images, clouds can interfere and compromise the quality of the maps. Therefore, images were collected for the summer season (December to February) so that cloud free images could be obtained. Also, as the aim is to analyse LST, therefore, it is more

logical to collect images for rain free summer days rather than cloudy and rainy winter days in Australia.

Landsat Level-1 data with precision and terrain correction (L1TP) images were collected, which provides radiometric and geodetic accuracy by incorporating ground control points while employing a Digital Elevation Model (DEM) for topographic displacement [45]. To cover land use from 1997, Landsat 5 (covering the year 1997), Landsat 7 (covering 1999 – 2013) and Landsat 8 (covering 2013 – 2020) L1TP images were collected from the Landsat image data access portal of U.S. geological survey (USGS) [46].

Considering the criteria for data collection and from available L1TP images, six years were selected (covering 23 years) for the time series LST analysis, which are 1997 (January), 2004 (February), 2007 (February), 2010 (January), 2016 (December) and 2020 (January).

Band 4 (Red), Band 5 (Near Infrared, NIR) and Band 10 (Thermal Infrared, TIRS) Landsat 8 images are specifically required for NDVI and LST analysis (demonstrated in Figure 5 in detail). The sample of Red, NIR and TIRS images are shown below in Figures 2–4. In the case of Landsat 4 to 7 images, Band 3, Band 4 and Band 6 images are required to represent Red, NIR and TIRS.

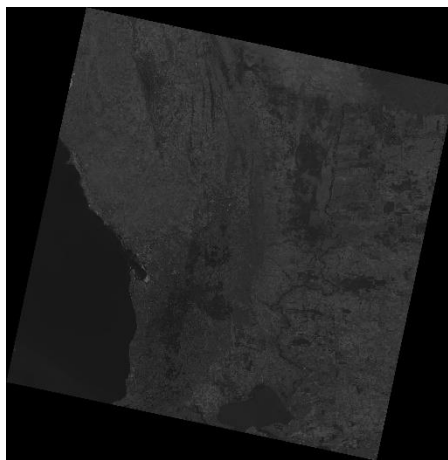


**Figure 2.** Band 4 (Red) Landsat 8 satellite image; wavelength ( $\mu\text{m}$ ) = 0.64-0.67, resolution (m) = 30 [46]. Image for the greater Adelaide region of South Australia captured on 02 January 2020.

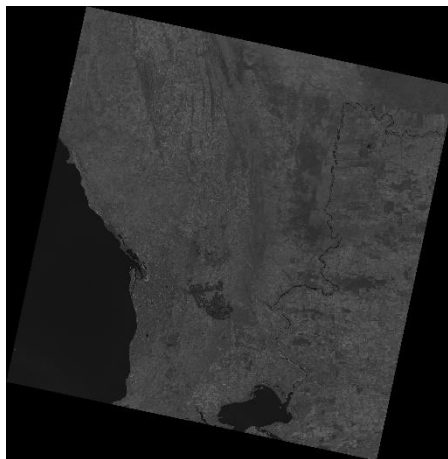


**Figure 3.** Band 5 (Near Infrared, NIR) Landsat 8 satellite image; wavelength ( $\mu\text{m}$ ) = 0.85-0.88, resolution (m) = 30 [46]. Image for the greater Adelaide region of South Australia captured on 02 January 2020.

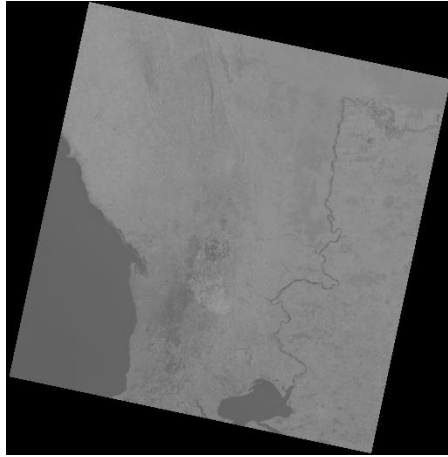


**Figure 4.** Band 10 (Thermal Infrared, TIRS) Landsat 8 satellite image; wavelength ( $\mu\text{m}$ ) = 10.6-11.19, resolution (m) = 100 [46]. Image for the greater Adelaide region of South Australia captured on 02 January 2020.

b. Meteorological data

Historical meteorological data for the City of Salisbury was collected from the Australian Bureau of Meteorology Department (BOM) [47]. These data facilitated a comparison between the LST and meteorological parameters (e.g. rainfall, solar exposure, air temperature etc.), denoting if the LST changes are linked to meteorological parameters.

c. Aerial photographs

In order to analyse the magnitude of land use impact on LST with greater precision, high-resolution aerial photographs for the study area were obtained from the government of South Australia's data portal [48]. A single aerial photograph was not used for analysing the degree of land use impact on LST, rather the aim was to support the results (land use/cover vs LST) obtained from Landsat data analysis with a high-resolution image for a particular year. These aerial photographs were captured with an aerial thermal sensor during the daytime of 23 March 2018 from ~3000 m altitude, with a 2m resolution. LiDAR (Light Detection and Ranging) remote sensing method was used for the photographs, especially for analysing urban heat islands of the Adelaide region.

### 2.3. Data Analysis

Land surface temperature (LST) and the normalised difference vegetation index (NDVI) can both be derived from Landsat imagery. LST is estimated using thermal infrared bands (Landsat 8 band 10), which detect the amount of radiation emitted by the Earth's surface. NDVI, on the other hand, is derived from the ratio of near-infrared and red reflectance bands (usually Landsat 8 bands 4 and 5).

Several steps were typically involved in deriving both LST and NDVI from a Landsat image. The first step was downloading the specific Landsat image bands. The images were then analysed through a series of formulas provided by USGS [49–51] and using the ArcMap raster calculation tool.

The estimated LST and NDVI spatial variations were further analysed to assess the trends and correlations between LST and other factors. First, 700 spatial points were randomly selected using the ArcMap from the City of Salisbury (Figure 6) to do the analysis. Then, the average of all points was compared with the meteorological parameters. NDVI impact on LST was analysed for each of the points.

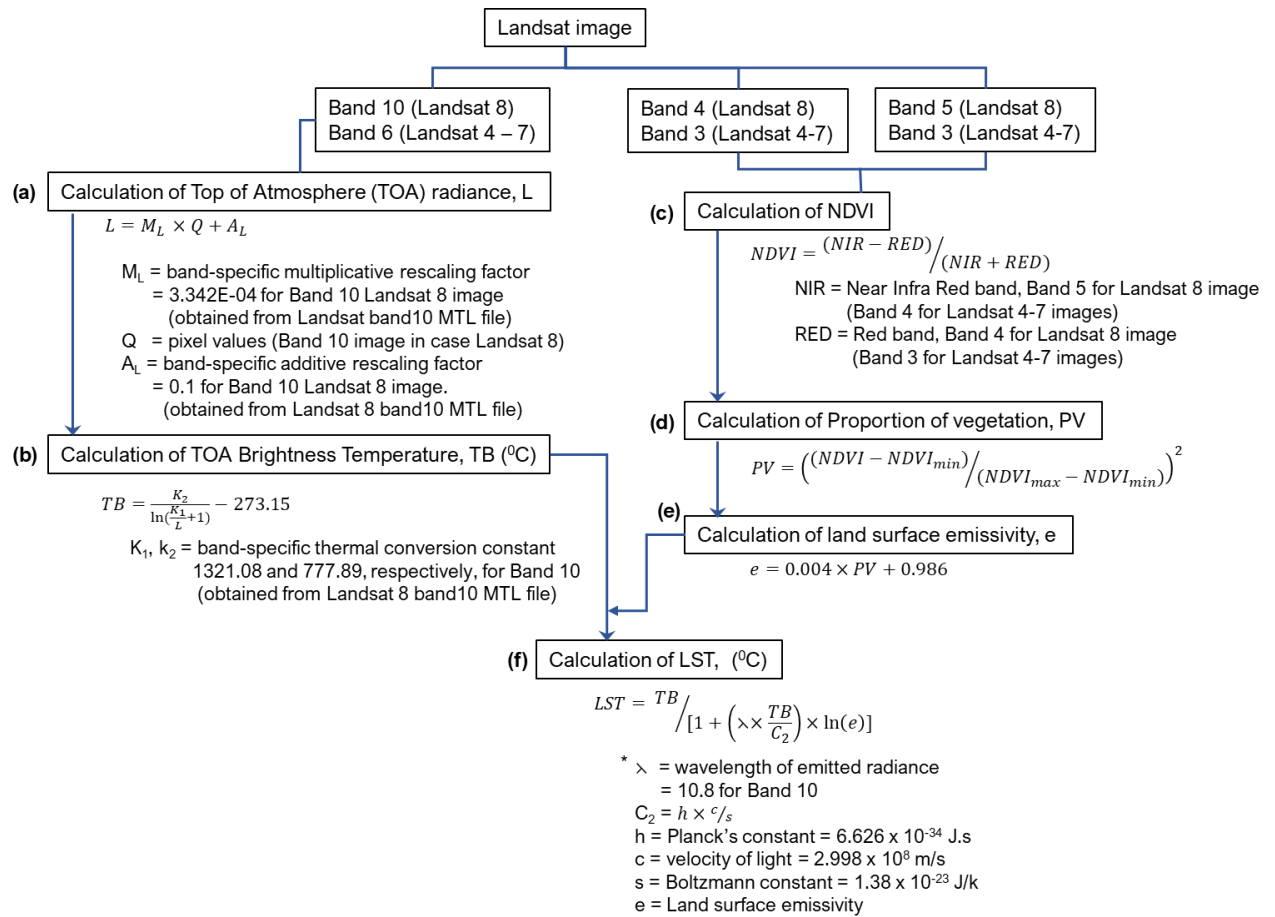


**Figure 5.** Schematic diagram of LST calculation from Landsat satellite image. References for calculation steps: **Steps (a)(b)** [49,52–54]; **Step (c)** [50–54]; **Steps (d)(e)** [51–54]; **Step (f)** [51,52,54]; \* Band 10 wavelength range 10.6–11.19  $\mu\text{m}$  [55], considered 10.8 for the calculation [52].

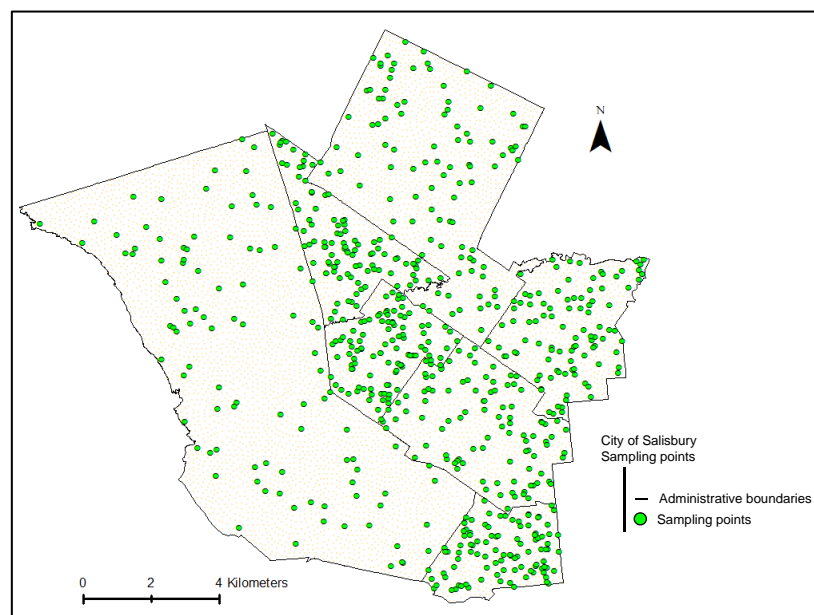


**Figure 6.** Randomised sampling points in the study area (City of Salisbury).

### 3. Results

As land use has been changing over the years in the study area, a changed vegetation pattern is also expected in the area. Analysis of the Normalised Difference Vegetation Index (NDVI) from Landsat images can portray those changes. Although Landsat images have a resolution of 60m (every pixel covers 60m x 60 m area), the analysis therefore cannot demonstrate every detail of the changes but can show the bigger picture in general. Figure 7 shows the analysis of NDVI for the study area since 1997, indicating a major shift from barren areas to bare soil, manifesting the development.

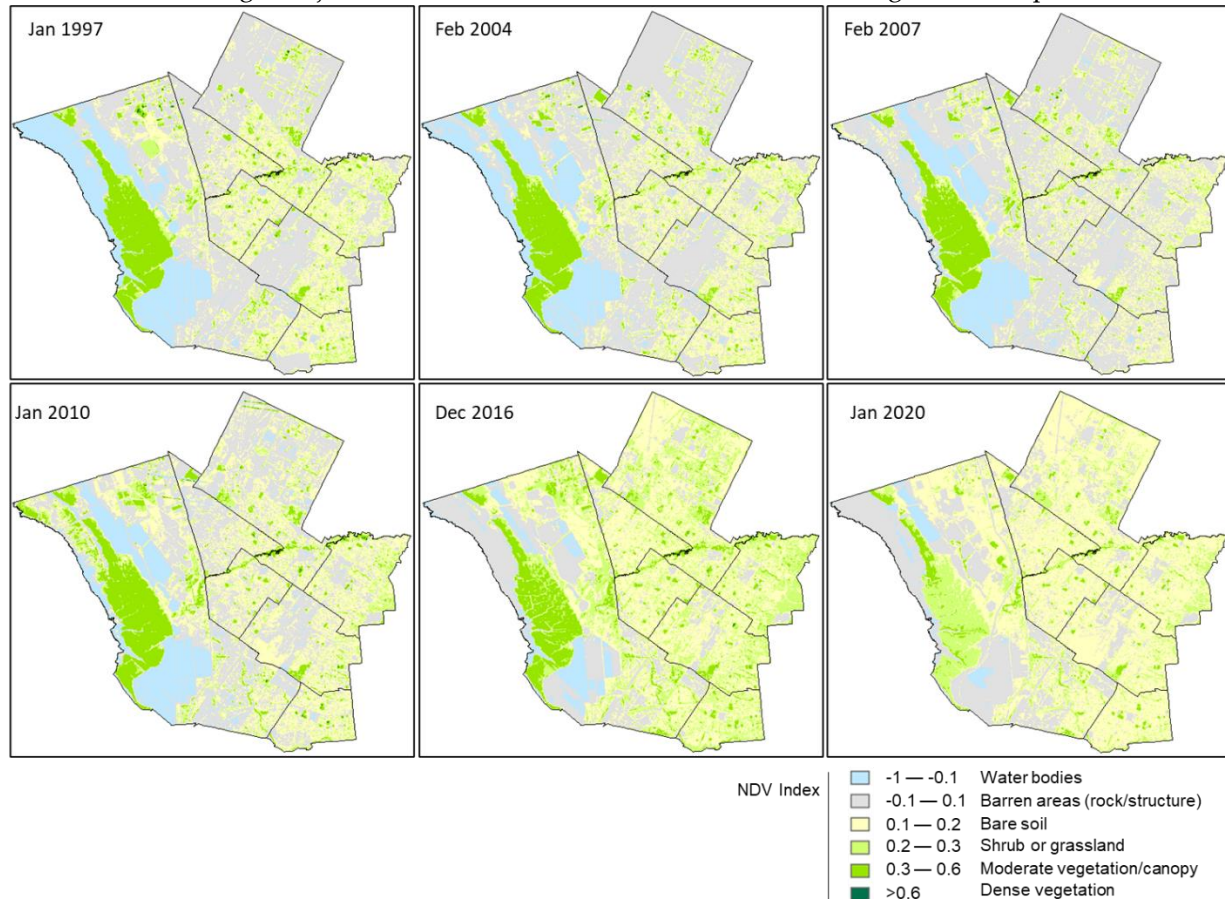


**Figure 7.** NDV Index (NDVI) over the years (1997-2020) for the City of Salisbury based on the Landsat satellite data. The interpretation of NDVI is obtained from NASA [56].

The NDV index in Figure 7 indicates the expansion of shrubs or grasslands over the study area, which is logically aligned with the development of urban grasslands (lawns, domestic gardens, vacant land, parks, etc.) with new developments. Therefore, the development of urban grasslands can be indicative of the increase in concrete structures as well along those areas. Increased bare soil land area compared to barren areas might support this assumption as well. A significant decrease in water bodies has been observed over the years, relating to a noticeable decrease in vegetation density. While moderate vegetation/canopy development was evident in some places over the years, especially roadside arboriculture, new developments (residential/commercial) also caused reduced vegetation/canopy density at many places. As the Landsat image has 60-m resolution, thus any detected change in vegetation through analysis correlates with a change over a large area, which is significant. This research intended to cross-check whether the NDVI analysis matches with the land use/land cover map, and found a compelling match, as shown in Figure 8. The comparison was done between 2020 Landsat NDVI analysis map with 2023 satellite land cover image as the 2020 land cover satellite image was not available and assuming the land cover pattern remains the same for 2020 and 2023. The approach was considered legitimate because the aim was to validate whether NDVI analysis done with Landsat images indicated a similar land cover pattern as is found in the satellite images.

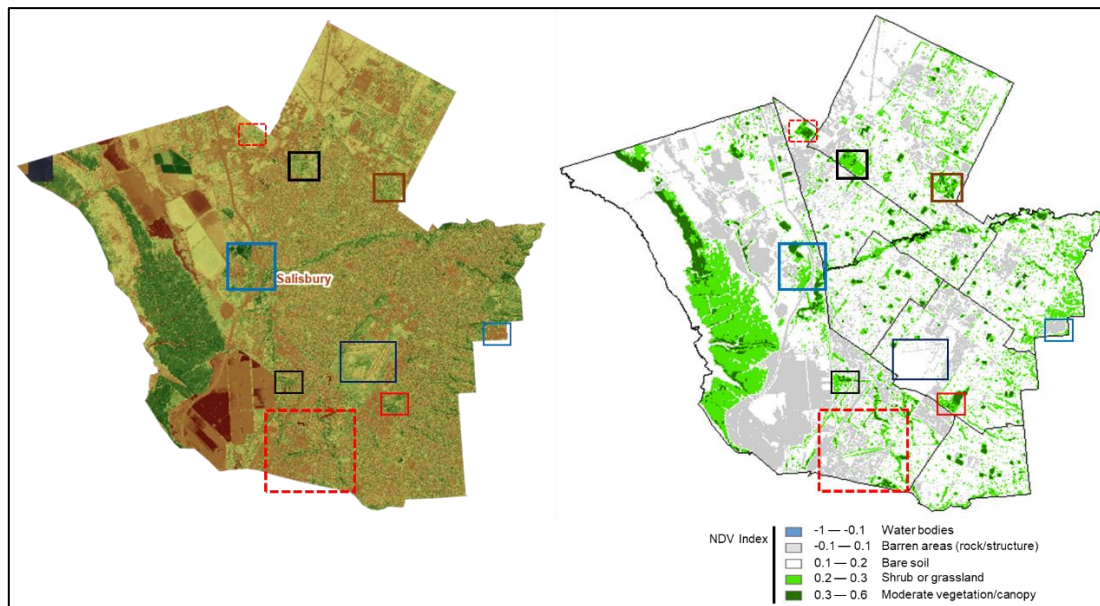


**Figure 8.** Comparison of NDVI analysis for 2020 with the 2023 satellite land cover image [43]. Similar coloured boxes indicate the same area for comparison.

Considering the land use and land cover changes over the years, the land surface temperature (LST) was analysed for the study area, depicting a consistent increase in the LST (Figure 9). The surface temperature was found to increase up to 5 °C in 23 years (1997 to 2003) at any location. However, 40-60 percentile of LST over the city, which indicates the average LST range, spanned between 32–33 °C to 39–39.6 °C (Figure 10a). If the top LST ranges are considered (more than 90 percentile of LST over the city), the range increased from 36–40 °C to 41–44.7 °C (Figure 10b). In both the cases, LST increased about 5–7 °C, indicating a consistent increase in LST throughout the study area, which might impact the liveability of the city as well as the ecological vulnerability.

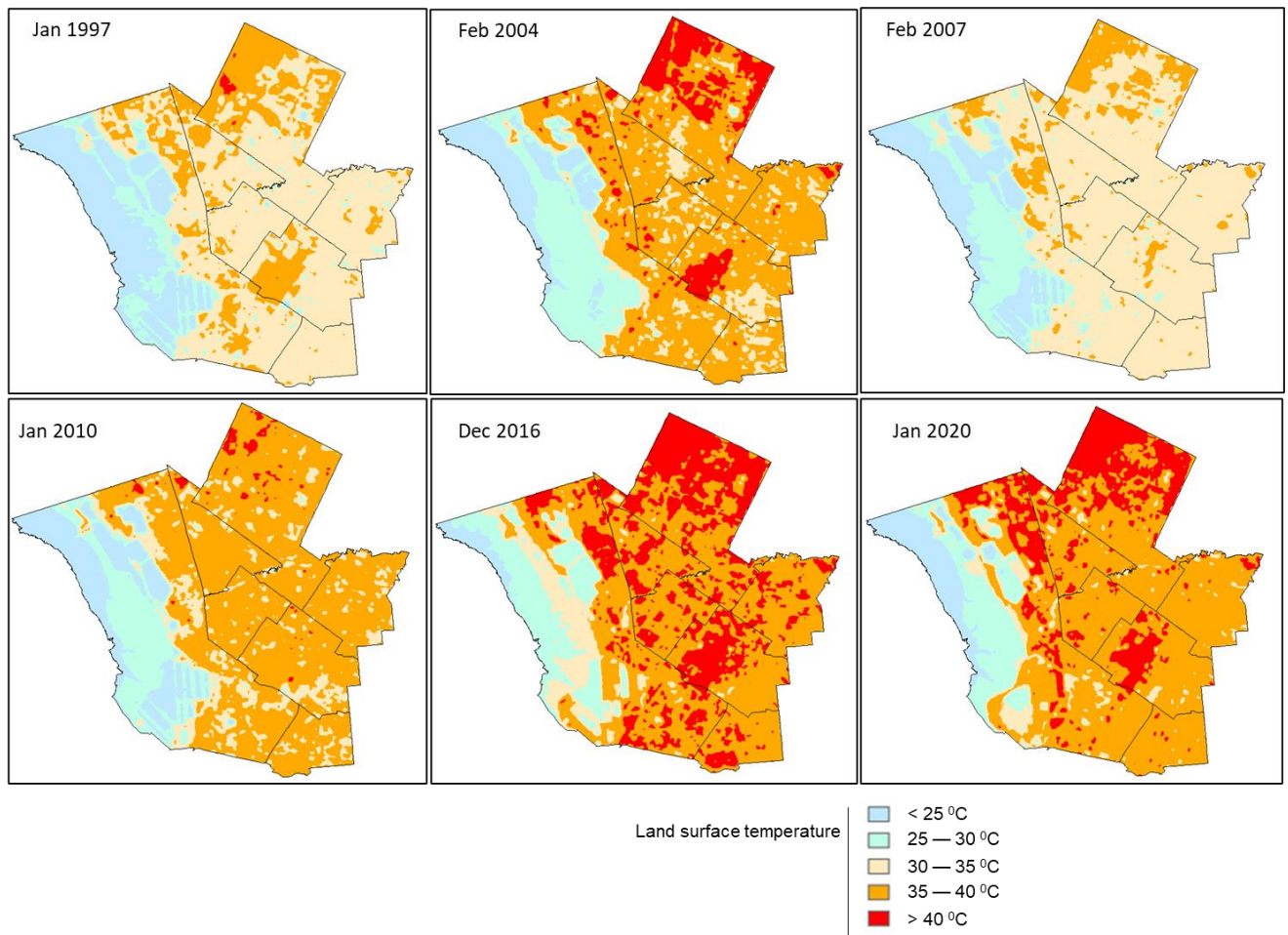


**Figure 9.** Estimated land surface temperature (LST) over the years (1997–2020) for the City of Salisbury based on the Landsat satellite data.

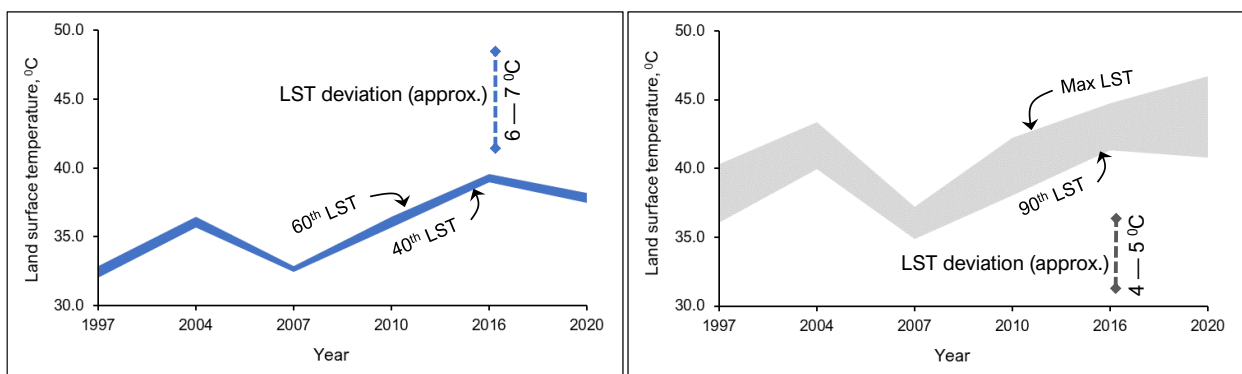


**Figure 10.** [a] 40–60 percentile of land surface temperature ( $^{\circ}$  C) range over the years for the City of Salisbury, Adelaide analysed from the Landsat satellite image data. [b] >90 percentile of land surface temperature ( $^{\circ}$  C) range (highest 10% range) over the years for the City of Salisbury, Adelaide analysed from the Landsat satellite image data.

The increase in LST can be correlated with climatic factors; LST was found to be increased with decreasing rainfall and NDVI [57]. As LST is the radiative temperature of land resulting from solar radiation [58], a correlation may exist between solar radiation data and increasing LST in the study area. Therefore, in this research, correlation analysis was conducted between LST and rainfall, air temperature and solar radiation data obtained from the local meteorological station for the selected

years. As the rainfall duration might affect the vegetation health, therefore, 3-months rainfall data (from the analysed satellite data) was considered to assess the correlation between rainfall and LST. The results are provided in Figure 11.

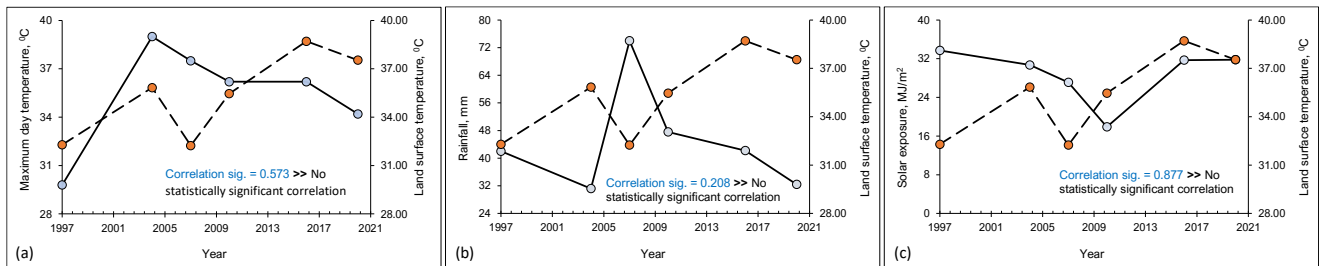


**Figure 11.** Correlation between Landsat analysed LST (dashed line) and (a) maximum day temperature, (b) 3-months total rainfall, and (c) solar exposure for the six selected years in the study area (City of Salisbury, Adelaide).

Results show that Landsat analysed LST is not statistically significantly correlated with the maximum air temperature ( $^{\circ}\text{C}$ ) of the analysis day and has a weak association (correlation coefficient 0.293) (Figure 11a). This means air temperature (or ambient temperature) had very little and statistically insignificant influence on the LST for the selected year. Rainfall showed a moderate level of negative correlation with the LST (correlation coefficient -0.6), which is expected as the rainfall might increase the vegetation to some extent, yet the association is not statistically significant (Figure 11b). That is, the level of change in rainfall during summertime couldn't significantly influence the change in LST over the study area. The correlation between solar exposure and LST was found to be the weakest (coefficient 0.082) and statically insignificant, meaning solar exposure barely had any influence on the LST (Figure 11c). A more detailed analysis for each year over a period of time might provide a more comprehensive correlation between LST and meteorological parameters. However, the current analysis depicts a lesser influence of the meteorological conditions on the LST. Therefore, the impact of land covers, especially the correlation of LST with NDVI was analysed for each concerned year, as presented in Figures 12 and 13.

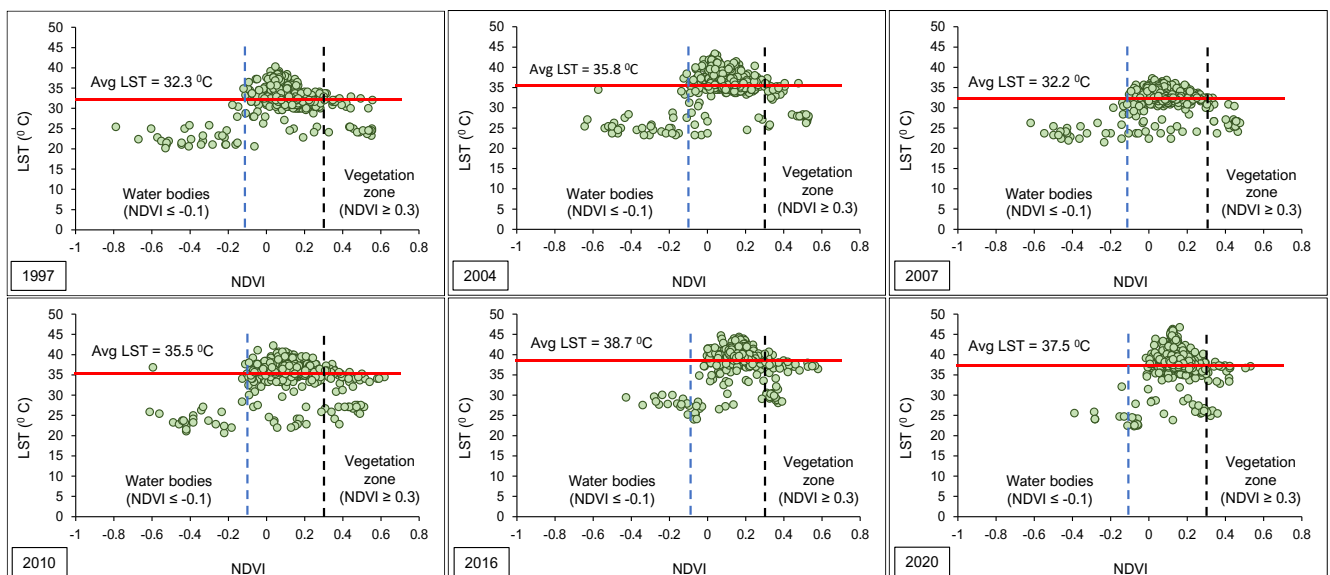


**Figure 12.** Year wise LST vs NDVI relationship for the six selected years in the study area (City of Salisbury, Adelaide).

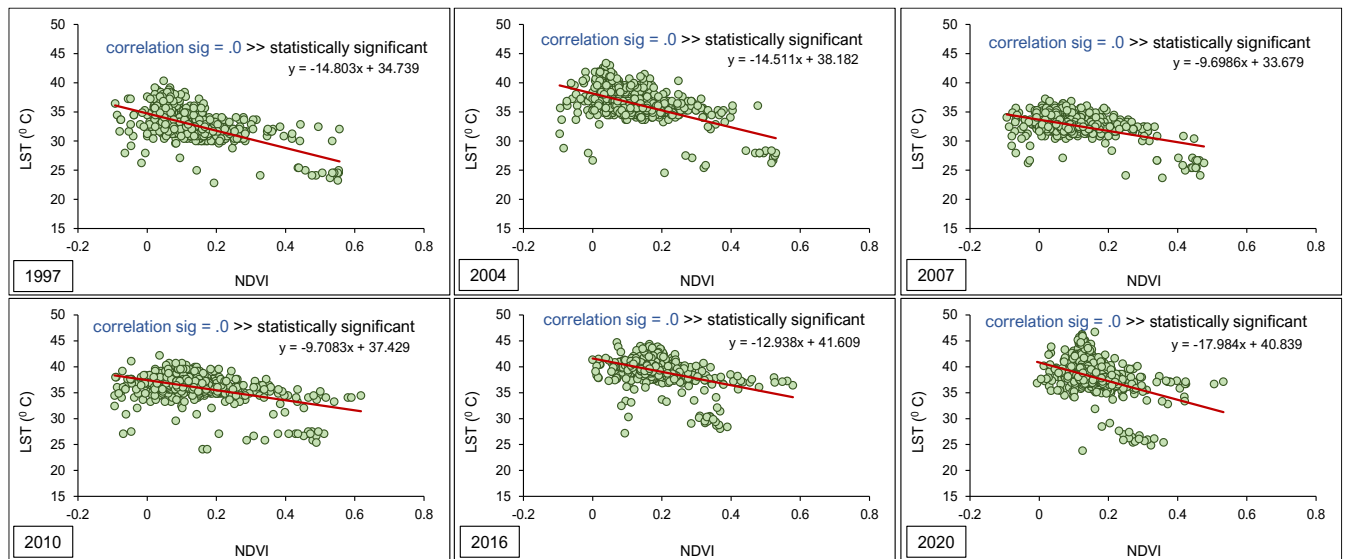


**Figure 13.** Year wise LST vs NDVI relationship for land areas (water body not considered) for the six selected years in the study area (City of Salisbury, Adelaide).

Figure 12 illustrates the analysis of LST versus NDVI, based on a random sample of 700 points within the study region. The findings indicate that regions without vegetation or with bare ground (NDVI values between -0.1 to 0.2) consistently experience elevated levels of LST and lack discernible differences from one another. The study consistently found that LST is low in areas with water bodies ( $\text{NDVI} \leq -0.1$ ) and regions with vegetation ( $\text{NDVI} \geq 0.3$ ). Compared to non-vegetative regions, areas with grasslands or shrubs demonstrated comparatively lower LST levels. The results imply that surface evapotranspiration and evaporation are significant factors that can effectively lower surface temperature.

The research aimed to examine the statistical significance of NDVI's correlation with LST across various years (only for land areas). As per the findings depicted in Figure 13, the results demonstrate that the correlation was statistically significant every year (moderate level of correlation in all the cases). This indicates that there is a significant decrease in LST with an increase in greenery in the study region. Further analysis shows that moderate vegetation or areas with widespread canopies can significantly lower the level of LST in urban regions compared to grasslands or shrub areas (Figure 14).

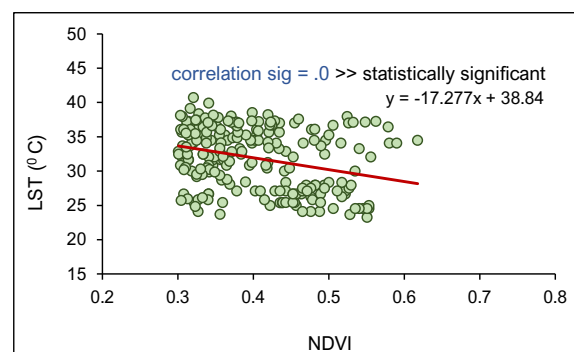


**Figure 14.** LST vs NDVI relationship for vegetative areas only (shrub or grassland or more) over more than 20 years.

Canopies reduce the amount of incoming solar radiation that reaches the ground, leading to lesser heat absorption by the ground surface. On the other hand, shrubs have an open canopy that permits more solar radiation to penetrate the ground, resulting in higher temperatures. Furthermore, canopies can enhance the evapotranspiration rate, which refers to the collective loss of water through

plant transpiration and soil evaporation. This mechanism contributes to the cooling of the surrounding environment, leading to a decrease in LST. The findings from the analysis corroborated the theoretical justification, thus lending legitimacy to the results obtained in this research.

Figure 15 provides additional spatial analysis that illustrates the impact of different land covers on LST. The results reveal that moderate vegetation or canopy cover can result in a temperature difference of at least 4 °C compared to areas with no vegetation (Box 1 in Figure 15). Non-vegetative land areas exhibit the highest temperature profile (Box 2). Depending on the type of land use, vegetation can lead to a temperature reduction ranging from 2 to 4 °C (Box 3). Furthermore, incorporating arboriculture along roads can potentially decrease the temperature by at least 1.5 °C compared to paved surfaces. Finally, dense canopies can effectively lower the land surface temperature even further (Box 4).

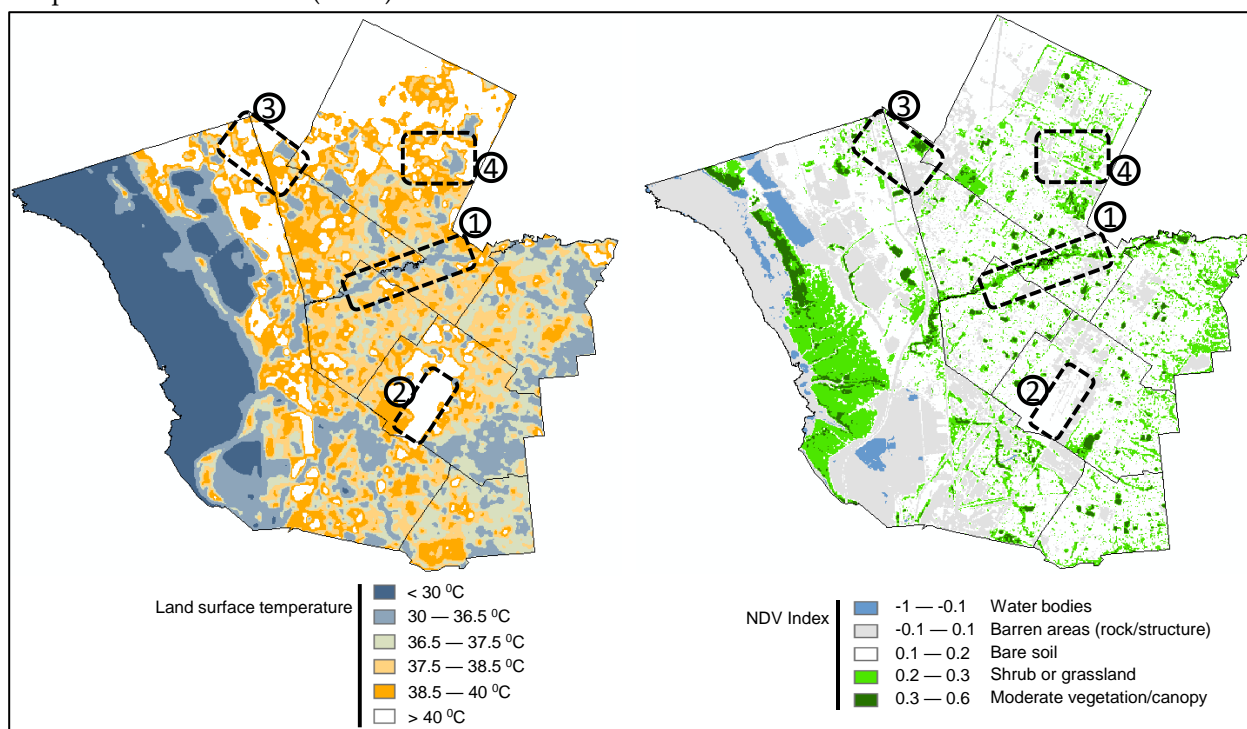


**Figure 15.** Change in LST compared to the change in NDVI values for the City of Salisbury based on the 2020 Landsat satellite data.

While the Landsat image analysis demonstrated the significant impact of canopy areas on the LST and showed the changes over the years, the magnitude of impact can be analysed more precisely with the aerial photographs (LiDAR image). This is because of the higher resolution (2 m) of LiDAR compared to Landsat images (30 m). Figure 16 shows the LST analysis with LiDAR and Landsat images and depicts a similar trend for the impact of vegetation on LST. However, the segmentation of LST in the LiDAR image is more detailed and the impact of each vegetation is accounted. Nevertheless, the comparison shows the acceptability of Landsat image analysis to predict the LST changes, especially for a wide region and for historical changes.

LiDAR image analysis shows that the vegetation can significantly reduce the LST by around 8—13 °C, depending on the surfaces (Figure 16). This is based on an image captured in March 2018 for the greater Adelaide region. Analysis shows that wherever the canopies are present, the LST remains around 33—34 °C, while wider roads and structures are found to increase LST above 40 °C. Road median strip arboriculture (with canopy >3m) is found to reduce LST in the middle of the wider roads, and so is found on narrow roads with dense arboriculture at the sides. Similarly, large structures are found to increase LST significantly.

Given the inevitability of urban development, the analysis recommends increasing the amount of greenery in order to mitigate the Land Surface Temperature (LST) in urban areas. Urban

arboriculture on both sides of roads might increase the density of greenery and thus would reduce the LST further.

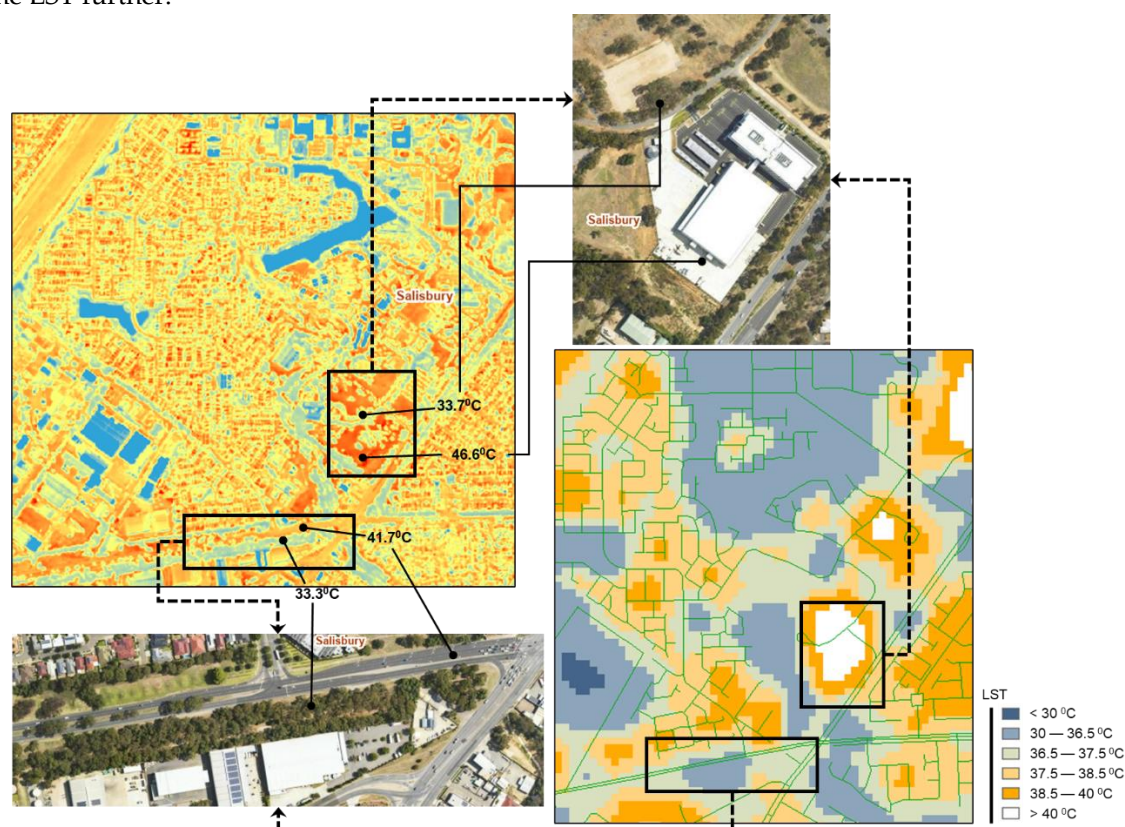


**Figure 16.** Variations of LST (against the land use) for the Mawson Lakes suburb in the City of Salisbury based on the 2018 aerial photographs (top left) [48] and analysed 2020 Landsat satellite data (bottom right).

## 5. Conclusions

As a developing city, the city of Salisbury demonstrated significant changes in land use over the years. Consequently, the land cover pattern has also changed, for instance, canopy density, urban arboriculture or paved surfaces. The research found a consistent increase in LST over the years for the study city, which is mainly correlated with the change in vegetation pattern (NDVI index). While no statistically significant influence of meteorological conditions was found on LST, rainfall might have some influence, especially in supporting vegetation growth. The research also shows that the density of vegetation or the presence of water bodies are significantly important factors in reducing the LST through the evapotranspiration process. Therefore, increasing urban arboriculture, especially moderate vegetation or canopies, is important to combat urban heat island effects with the growing need for urban development. The research outcome is based on low-resolution Landsat images, which have shown a significant correlation. However, further research on higher resolution remote sensing data might contribute to assessing the extent of the effect of different management strategies to control urban heat island effects.

**Author Contributions:** Conceptualization, A.I., M.M.R. and C.C.; methodology, A.I. and M.M.R.; software, A.I.; validation, M.M.R., C.C. and P.L.; formal analysis, A.I. and M.M.R.; resources, C.C. and P.L.; writing—original draft preparation, A.I. and M.M.R.; writing—review and editing, C.C. and P.L.; visualisation, A.I.; supervision, M.M.R.; project administration, C.C. and P.L. All authors have read and agreed to the published version of the manuscript.

**Funding:** This research received no external funding.

**Data Availability Statement:** Publicly available datasets were analysed in this study.

**Conflicts of Interest:** The authors declare no conflict of interest.

## References

1. Yang, L., F. Qian, D.-X. Song, and K.-J. Zheng, *Research on Urban Heat-Island Effect*. Procedia Engineering, 2016. **169**: p. 11-18.
2. Rashid, N., J.A.M.M. Alam, M.A. Chowdhury, and S.L.U. Islam, *Impact of landuse change and urbanization on urban heat island effect in Narayanganj city, Bangladesh: A remote sensing-based estimation*. Environmental Challenges, 2022. **8**: p. 100571.
3. Yang, C., X. He, F. Yan, L. Yu, K. Bu, J. Yang, L. Chang, and S. Zhang, *Mapping the Influence of Land Use/Land Cover Changes on the Urban Heat Island Effect—A Case Study of Changchun, China*. Sustainability, 2017. **9**(2): p. 312.
4. Buo, I., V. Sagris, I. Burdun, and E. Uuemaa, *Estimating the expansion of urban areas and urban heat islands (UHI) in Ghana: a case study*. Natural Hazards, 2021. **105**(2): p. 1299-1321.
5. Jadraque Gago, E., S. Etxebarria Berrizbeitia, R. Pacheco Torres, and T. Muneer, *Effect of Land Use/Cover Changes on Urban Cool Island Phenomenon in Seville, Spain*. Energies, 2020. **13**(12): p. 3040.
6. Lee, P.S.-H. and J. Park, *An Effect of Urban Forest on Urban Thermal Environment in Seoul, South Korea, Based on Landsat Imagery Analysis*. Forests, 2020. **11**(6): p. 630.
7. Kim, M., D. Kim, and G. Kim, *Examining the Relationship between Land Use/Land Cover (LULC) and Land Surface Temperature (LST) Using Explainable Artificial Intelligence (XAI) Models: A Case Study of Seoul, South Korea*. International Journal of Environmental Research and Public Health, 2022. **19**(23): p. 15926.
8. Xiong, Y., F. Peng, and B. Zou, *Spatiotemporal influences of land use/cover changes on the heat island effect in rapid urbanization area*. Frontiers of Earth Science, 2019. **13**(3): p. 614-627.
9. Zhou, S., K. Wang, S. Yang, W. Li, Y. Zhang, B. Zhang, Y. Fu, X. Liu, Y. Run, O.G. Chubwa, G. Zhao, J. Dong, and Y. Cui, *Warming Effort and Energy Budget Difference of Various Human Land Use Intensity: Case Study of Beijing, China*. Land, 2020. **9**(9): p. 280.
10. Huang, Q., J. Huang, X. Yang, C. Fang, and Y. Liang, *Quantifying the seasonal contribution of coupling urban land use types on Urban Heat Island using Land Contribution Index: A case study in Wuhan, China*. Sustainable Cities and Society, 2019. **44**: p. 666-675.
11. Feng, H., X. Zhao, F. Chen, and L. Wu, *Using land use change trajectories to quantify the effects of urbanization on urban heat island*. Advances in Space Research, 2014. **53**(3): p. 463-473.
12. Yao, L., S. Sun, C. Song, J. Li, W. Xu, and Y. Xu, *Understanding the spatiotemporal pattern of the urban heat island footprint in the context of urbanization, a case study in Beijing, China*. Applied Geography, 2021. **133**: p. 102496.
13. Wang, J., B. Huang, D. Fu, P.M. Atkinson, and X. Zhang, *Response of urban heat island to future urban expansion over the Beijing–Tianjin–Hebei metropolitan area*. Applied Geography, 2016. **70**: p. 26-36.
14. Chun, B. and J.-M. Guldmann, *Impact of greening on the urban heat island: Seasonal variations and mitigation strategies*. Computers, Environment and Urban Systems, 2018. **71**: p. 165-176.
15. Sun, Q., Z. Wu, and J. Tan, *The relationship between land surface temperature and land use/land cover in Guangzhou, China*. Environmental Earth Sciences, 2012. **65**(6): p. 1687-1694.
16. Wang, L. and S.W. Zhang, *ANALYSIS ON THE RELATIONSHIP BETWEEN THE PATTERN OF GREEN SPACES AND LAND SURFACE TEMPERATURE BASED ON NORMALIZED DIFFERENCE VEGETATION INDEX: A CASE STUDY IN CHANGCHUN CITY, CHINA*. Fresenius Environmental Bulletin, 2015. **24**(8): p. 2444-2451.
17. Yue, W., J. Xu, W. Tan, and L. Xu, *The relationship between land surface temperature and NDVI with remote sensing: application to Shanghai Landsat 7 ETM+ data*. International Journal of Remote Sensing, 2007. **28**(15): p. 3205-3226.
18. Kamali Maskooni, E., H. Hashemi, R. Berndtsson, P. Daneshkar Arasteh, and M. Kazemi, *Impact of spatiotemporal land-use and land-cover changes on surface urban heat islands in a semiarid region using Landsat data*. International Journal of Digital Earth, 2021. **14**(2): p. 250-270.
19. Fan, C., S.W. Myint, S. Kaplan, A. Middel, B. Zheng, A. Rahman, H.-P. Huang, A. Brazel, and D.G. Blumberg, *Understanding the Impact of Urbanization on Surface Urban Heat Islands—A Longitudinal Analysis of the Oasis Effect in Subtropical Desert Cities*. Remote Sensing, 2017. **9**(7): p. 672.
20. Park, Y., J.-M. Guldmann, and D. Liu, *Impacts of tree and building shades on the urban heat island: Combining remote sensing, 3D digital city and spatial regression approaches*. Computers, Environment and Urban Systems, 2021. **88**: p. 101655.

21. Arshad, S., S.R. Ahmad, S. Abbas, A. Asharf, N.A. Siddiqui, and Z.u. Islam, *Quantifying the contribution of diminishing green spaces and urban sprawl to urban heat island effect in a rapidly urbanizing metropolitan city of Pakistan*. *Land Use Policy*, 2022. **113**: p. 105874.
22. Dissanayake, D., T. Morimoto, M. Ranagalage, and Y. Murayama, *Land-Use/Land-Cover Changes and Their Impact on Surface Urban Heat Islands: Case Study of Kandy City, Sri Lanka*. *Climate*, 2019. **7**(8): p. 99.
23. Tong, S., J. Prior, G. McGregor, X. Shi, and P. Kinney, *Urban heat: an increasing threat to global health*. *BMJ*, 2021. **375**: p. n2467.
24. Piracha, A. and M.T. Chaudhary, *Urban Air Pollution, Urban Heat Island and Human Health: A Review of the Literature*. *Sustainability*, 2022. **14**(15): p. 9234.
25. Singh, N., S. Singh, and R.K. Mall, *Chapter 17 - Urban ecology and human health: implications of urban heat island, air pollution and climate change nexus*, in *Urban Ecology*, P. Verma, et al., Editors. 2020, Elsevier. p. 317-334.
26. Conti, S., M. Masocco, P. Meli, G. Minelli, E. Palummeri, R. Solimini, V. Toccaceli, and M. Vichi, *General and specific mortality among the elderly during the 2003 heat wave in Genoa (Italy)*. *Environmental Research*, 2007. **103**(2): p. 267-274.
27. Ho, J.Y., Y. Shi, K.K.L. Lau, E.Y.Y. Ng, C. Ren, and W.B. Goggins, *Urban heat island effect-related mortality under extreme heat and non-extreme heat scenarios: A 2010–2019 case study in Hong Kong*. *Science of The Total Environment*, 2023. **858**: p. 159791.
28. Sheridan, S.C., C.C. Lee, and M.J. Allen, *The Mortality Response to Absolute and Relative Temperature Extremes*. *International Journal of Environmental Research and Public Health*, 2019. **16**(9): p. 1493.
29. Wang, J., Z. Xiang, W. Wang, W. Chang, and Y. Wang, *Impacts of strengthened warming by urban heat island on carbon sequestration of urban ecosystems in a subtropical city of China*. *Urban Ecosystems*, 2021. **24**(6): p. 1165-1177.
30. Corumluoglu, O. and I. Asri, *The effect of urban heat island on Izmir's city ecosystem and climate*. *Environmental Science and Pollution Research*, 2015. **22**(5): p. 3202-3211.
31. Ding, F., H. Pang, and W. Guo, *Impact of the urban heat island on residents' energy consumption: a case study of Qingdao*. *IOP Conference Series: Earth and Environmental Science*, 2018. **121**(3): p. 032026.
32. Zhou, Y., Z. Zhuang, F. Yang, Y. Yu, and X. Xie, *Urban morphology on heat island and building energy consumption*. *Procedia Engineering*, 2017. **205**: p. 2401-2406.
33. Li, X., Y. Zhou, S. Yu, G. Jia, H. Li, and W. Li, *Urban heat island impacts on building energy consumption: A review of approaches and findings*. *Energy*, 2019. **174**: p. 407-419.
34. Abuzar, M., A. McAllister, D. Whitfield, and K. Sheffield, *Remotely-Sensed Surface Temperature and Vegetation Status for the Assessment of Decadal Change in the Irrigated Land Cover of North-Central Victoria, Australia*. *LAND*, 2020. **9**(9).
35. Chen, B., G. Xu, N.C. Coops, P. Ciais, and R.B. Myneni, *Satellite-observed changes in terrestrial vegetation growth trends across the Asia-Pacific region associated with land cover and climate from 1982 to 2011*. *International Journal of Digital Earth*, 2016. **9**(11): p. 1055-1076.
36. Narisma, G.T. and A.J. Pitman, *The Impact of 200 Years of Land Cover Change on the Australian Near-Surface Climate*. *Journal of Hydrometeorology*, 2003. **4**(2): p. 424-436.
37. Chen, H., Q. Deng, Z. Zhou, Z. Ren, and X. Shan, *Influence of land cover change on spatio-temporal distribution of urban heat island —a case in Wuhan main urban area*. *Sustainable Cities and Society*, 2022. **79**: p. 103715.
38. Teimouri, R., R. Ghorbani, P. Karbasi, and E. Sharifi, *Investigation of land use changes using the landscape ecology approach in Maragheh City, Iran*. *Journal of Environmental Studies and Sciences*, 2023.
39. Liu, L. and Y. Zhang, *Urban Heat Island Analysis Using the Landsat TM Data and ASTER Data: A Case Study in Hong Kong*. *Remote Sensing*, 2011. **3**(7): p. 1535-1552.
40. Yee, M. and J.O. Kaplan, *Drivers of urban heat in Hong Kong over the past 116 years*. *Urban Climate*, 2022. **46**: p. 101308.
41. Dihkan, M., F. Karsli, A. Guneroglu, and N. Guneroglu, *Revisiting Urban Heat Island Effects in Coastal Regions: Mitigation Strategies for the Megacity of Istanbul*, in *Urban Heat Island (UHI) Mitigation: Hot and Humid Regions*, N. Enteria, M. Santamouris, and U. Eicker, Editors. 2021, Springer Singapore: Singapore. p. 277-307.
42. CoS. *About our City of Salisbury- quick facts*. 2023 [cited 2023 26 April]; Available from: <https://www.salisbury.sa.gov.au/council/about-our-city-of-salisbury/quick-facts>.

43. GoogleMaps. *Salisbury, South Australia*. 2023 [cited 2023 26 April]; Available from: <https://www.google.com/maps/place/Salisbury,+SA/@-34.8333696,138.6928723,11z/data=!4m6!3m5!1s0x6ab0b12e3cda0511:0x69869588a94a402a!8m2!3d-34.7602947!4d138.6188423!16zL20vMDZsM2Ri>.
44. PlanSA. *Development plan map*. 2019 [cited 2022 26 March]; Available from: [https://plan.sa.gov.au/data/assets/pdf\\_file/0012/744978/Consultation\\_change\\_maps\\_-\\_Salisbury.pdf](https://plan.sa.gov.au/data/assets/pdf_file/0012/744978/Consultation_change_maps_-_Salisbury.pdf).
45. USGS. *Landsat levels of processing*. 2023 [cited 2023 26 April]; Available from: <https://www.usgs.gov/landsat-missions/landsat-levels-processing>.
46. USGS. *Earth explorer*. 2023 [cited 2022 15 Jun]; Available from: <https://earthexplorer.usgs.gov/>.
47. BOM. *Climate data online*. 2022 [cited 2022 12 Jan]; Available from: <http://www.bom.gov.au/climate/data/index.shtml>.
48. DEW. *Urban heat mapping viewer*. 2021 [cited 2022 12 June]; Available from: <http://spatialwebapps.environment.sa.gov.au/urbanheat/?viewer=urbanheat&runWorkflow=StartupResilientEast>.
49. USGS. *Using the USGS Landsat level-1 data product*. 2023 [cited 2023 26 April]; Available from: <https://www.usgs.gov/landsat-missions/using-usgs-landsat-level-1-data-product>.
50. USGS. *Landsat Normalized Difference Vegetation Index*. 2023 [cited 2023 26 April]; Available from: <https://www.usgs.gov/landsat-missions/landsat-normalized-difference-vegetation-index#:~:text=In%20Landsat%20%2D7%2C%20NDVI,Band%20%20%2B%20Band%204>.
51. USGS. *Landsat collection 2 surface temperature*. 2023 [cited 2023 26 April]; Available from: <https://www.usgs.gov/landsat-missions/landsat-collection-2-surface-temperature>.
52. Avdan, U. and G. Jovanovska, *Algorithm for Automated Mapping of Land Surface Temperature Using LANDSAT 8 Satellite Data*. *Journal of Sensors*, 2016. **2016**: p. 1480307.
53. Sajib, M.Q.U. and T. Wang, *Estimation of land surface temperature in an agricultural region of bangladesh from landsat 8: Intercomparison of four algorithms*. *Sensors (Basel)*, 2020. **20**(6).
54. Sahani, N., *Assessment of spatio-temporal changes of land surface temperature (LST) in Kanchenjunga Biosphere Reserve (KBR), India using Landsat satellite image and single channel algorithm*. *Remote Sensing Applications: Society and Environment*, 2021. **24**: p. 100659.
55. USGS. *What are the band designations for the Landsat satellites?* 2023 [cited 2023 26 April]; Available from: <https://www.usgs.gov/faqs/what-are-band-designations-landsat-satellites>.
56. NASA. *Measuring vegetation (NDVI & EVI)*. 2000 [cited 2022 24 Feb]; Available from: <https://earthobservatory.nasa.gov/features/MeasuringVegetation>.
57. Garai, S., M. Khatun, R. Singh, J. Sharma, M. Pradhan, A. Ranjan, S.M. Rahaman, M.L. Khan, and S. Tiwari, *Assessing correlation between Rainfall, normalized difference Vegetation Index (NDVI) and land surface temperature (LST) in Eastern India*. *Safety in Extreme Environments*, 2022. **4**(2): p. 119-127.
58. Khan, A., S. Chatterjee, and Y. Weng, *2 - Characterizing thermal fields and evaluating UHI effects*, in *Urban Heat Island Modeling for Tropical Climates*, A. Khan, S. Chatterjee, and Y. Weng, Editors. 2021, Elsevier. p. 37-67.

**Disclaimer/Publisher's Note:** The statements, opinions and data contained in all publications are solely those of the individual author(s) and contributor(s) and not of MDPI and/or the editor(s). MDPI and/or the editor(s) disclaim responsibility for any injury to people or property resulting from any ideas, methods, instructions or products referred to in the content.